LITERATURE CITED

1. Yu. P. Raizer, "On the deceleration and transformation of energy of a plasma expanding in a vacuum magnetic field" [in Russian], Zh. Prikl. Mekh. Tekh. Fiz., No. 6 (1963).
2. V. A. Pilipenko, "On the form of the boundary of a freely expanding plasma in a magnetic field," [in Russian], Zh. Prikl. Mekh. Tekh. Fiz., No. 2, (1967).
3. J. W. Poukey, "Expansion of a plasma shell into a vacuum magnetic field," Phys. Fluids, 12, No. 7 (1969).
4. S. M. Bakhrakh, E. V. Gubkov, et al., "Expansion of a plasma cloud in a uniform magnetic field" [in Russian], Zh. Prikl. Mekh. Tekh. Fiz., No. 4, (1974).
5. S. A. Colgate, "The phenomenology of the mass motion of a high altitude nuclear explosion," J. Geophys. Research, 70, No. 13 (1965).
6. V. P. Korobeinikov, "Problems in the theory of a point explosion in a gas" [in Russian], Trudy MI Akad. Nauk SSSR, No. CXIX (1973).
7. A. I. Golubev, A. A. Solov'ev, and V. A. Terekhin, "On the collisionless expansion of an ionized cloud in a uniform plasma in a magnetic field" [in Russian], Zh. Prikl. Mekh. Tekh. Fiz., No. 5 (1978).
8. G. F. Chew, M. L. Goldberger, and F. E. Low, "The Boltzmann equation and the one-fluid hydromagnetic equations in the absence of particle collisions," Proc. Roy. Soc., A236, 112 (1956).
9. D. W. Forslund and J. P. Friedberg, "Theory of laminar collisionless shocks," Phys. Rev. Lett., 27, No. 18 (1971).
10. R. A. Chodura, "Hybrid fluid-particle model of ion heating in high Mach number shock waves," Nucl. Fusion, 15, 55 (1975).
11. A. G. Sgro and C. W. Nielson, "Hybrid model studies of ion dynamics and magnetic field diffusion during pinch implosion," Phys. Fluids, 19, No. 1, (1976).
12. A. I. Golubev and A. A. Solov'ev, "Algorithms for the numerical solution of strong explosions in a dilute plasma" [in Russian], ChMMSS, 10, No. 4 (1979).

CHARACTERISTICS OF THE STEADY-STATE FLOW OF A TWO-TEMPERATURE ARGON-ARC PLASMA IN A CHANNEL

V. S. Klubnikin, V. A. Laptev, and A. A. Salangin

UDC 533.915.072

Design of high-temperature gas heaters with given characteristics is hindered by the lack of applicable models closely adapted to real conditions. This applies particularly to electric-arc plasma sources that produce thermally nonequilibrium plasma. Theoretical studies have been made [1-6] of the arc characteristics in the two-temperature approximation for the initial and steady-state parts. However, most of these are restricted to arc burning in the absence of a flow [1, 3] and laminar gas flow in the discharge channel [2, 4, 5], while in [4] the calculations were performed with a very crude approximation in order to obtain a simple solution. The most accurate analysis is to be found in [2, 5], while in [6] there is an estimate of the effects from turbulence. No detailed analysis has been made of the effects of the transition from laminar flow to turbulent on the characteristics of a two-temperature flow of electric-arc plasma. Also, the properties of the plasma have been derived from formulas that are not always reliable, which substantially hinders examination of the accuracy and applicability of the results.

We have examined the effects of laminar and turbulent flow on the characteristics of a two-temperature argon plasma in the steady-state part of an electric arc in a cylindrical channel. We have examined the existing formulas for the plasma properties and have selected those that agree best with experiment.

It has been found that the following system of equations can be used to describe the phenomena occurring in an electric arc stabilized by the walls of a cylindrical channel and bearing a longitudinal gas flow:

Leningrad. Translated from Zhurnal Prikladnoi Mekhaniki i Tekhnicheskoi Fiziki, No. 5, pp. 17-24, September-October, 1983. Original article submitted August 9, 1982.

 0021-8944/83/2405-0620$07.50

1) the energy equation for the electron gas

$$\sigma E^2 = 3\frac{m_e}{m_a} n_e \nu k (T_e - T) - \frac{1}{r}\frac{d}{dr}\left(r\lambda_e \frac{dT_e}{dr}\right) - \frac{1}{r}\frac{d}{dr}\left[r\left(\frac{3}{2}kT_e + E_i\right) D_a \frac{dn_e}{dr}\right] + W_r; \quad (1)$$

2) the energy equation for the atomic-ionic gas

$$3\frac{m_e}{m_a} n_e \nu k (T_e - T) = -\frac{1}{r}\frac{d}{dr}\left[r(\lambda + \lambda_T)\frac{dT}{dr}\right]; \quad (2)$$

3) the equation of motion

$$\frac{1}{r}\frac{d}{dr}\left[r(\eta + \eta_T)\frac{du}{dr}\right] = \frac{dp}{dz}, \quad (3)$$

where T_e, m_e, n_e, λ_e are the electron temperature, mass, concentration, and thermal conductivity, T, m_a, and λ are the temperature, mass, and thermal conductivity of the atoms and ions, σ is the plasma electrical conductivity, ν is the effective frequency of the elastic collisions between electrons and atoms or ions, E is the electric field strength, E_i is the ionization energy, D_a is the ambipolar diffusion coefficient, W_r is the radiated power, k is Boltzmann's constant, η_T and λ_T are the turbulent viscosity and thermal conductivity, η is the dynamic viscosity, dp/dz is the longitudinal static-pressure gradient, and u is the longitudinal component of the plasma velocity.

The boundary conditions for (1)-(3) take the form

$$\text{at } r = 0 \quad dT_e/dr = dT/dr = dn_e/dr = du/dr = 0; \quad (4)$$

$$\text{at } r = R \quad T = T_R, \; u = 0, \; T_e = T_{eR}. \quad (5)$$

T_R for the atomic-ionic gas was taken as 300°K, while T_{eR} for the electron component was found from (1) on the assumption that all the energy σE^2 supplied to the electrons in the part of the plasma near the wall is transferred to the atoms and ions by elastic collision, so

$$T_{eR} = (T + m_a \sigma E^2/(3m_e n_e \nu k))|_{r=R}.$$

Particular attention was given to choosing the formulas for the plasma properties. Comparison with experimental data and approximate calculations give the collision cross sections and transport coefficients from the following formulas (Te, T, K; n_e, n_a, cm^{-3}):

1) the effective cross section for elastic electron-atom collisions [7]

$$Q_{ea} = (0.1 + 3.6\cdot 10^{-4} T_e)\cdot 10^{-16} \text{ cm}^{-2};$$

2) the effective cross section for electron-ion collisions [8]

$$Q_{ei} = \frac{20.2\cdot 10^{-6}}{T_e^2} \lg\left[\frac{279 T_e}{n_e^{1/3}}\left(\frac{T}{T_e + T}\right)^{1/3}\right], \text{ cm}^2;$$

3) the effective elastic-collision frequency

$$\nu = \sqrt{\frac{8kT_e}{\pi m_e}}(n_e Q_{ei} + n_a Q_{ea}), \text{ 1/sec},$$

where n_a is the atom concentration;

4) the electrical conductivity of the weakly ionized gas [9]

$$\sigma_1 = 1.37\cdot 10^{-23} \frac{n_e\left(\sqrt{\frac{T_e}{m_e}} + \sqrt{\frac{T}{m_a}}\right)}{T_e Q_{ea}(n_e + n_a)};$$

5) the electrical conductivity of the completely ionized gas [10]

$$\sigma_2 = \frac{6.67\cdot 10^{-5} T_e^{3/2}}{\lg\left[\dfrac{1.24\cdot 10^4 T_e^{3/2}}{n_e^{1/2}}\right]},\ \text{Sm/cm};$$

6) the thermal conductivity of the electrons in the weakly ionized gas [11]

$$\lambda_{e1} = \frac{5.65\cdot 10^{-18} T_e^{1/2} n_e}{n_a Q_{ea}},\quad \text{W/(cm}\cdot\text{°K)}$$

7) the thermal conductivity of the electrons in a completely ionized plasma [9]

$$\lambda_{e2} = \frac{1.84\cdot 10^{-12} T_e^{5/2}}{\ln\left[\dfrac{1.24\cdot 10^4 T_e^{3/2}}{n_e^{1/2}}\right]},\quad \text{W/(cm}\cdot\text{°K)}$$

8) the electrical conductivity and thermal conductivity of the electrons in a partially ionized plasma

$$\sigma = \sigma_1\sigma_2/(\sigma_1 + \sigma_2),\ \lambda_e = \lambda_{e1}\lambda_{e2}/(\lambda_{e1} + \lambda_{e2});$$

9) the thermal conductivity of the atoms and ions

$$\lambda = 2.53\cdot 10^{-6} T^{0.744} n_a/(n_a + 3.14 n_e),\quad \text{W/(cm}\cdot\text{°K)}$$

This formula agrees well with experiment: The ambipolar diffusion coefficient [7, 12] is $D_a = 4.05\cdot 10^{-0.63}(T_e + T)$ cm^2/sec. The plasma composition was calculated from Saha's formula and the equation of state for a quasineutral plasma.

The turbulent viscosity and thermal conductivity were calculated in accordance with Prandtl's hypothesis on the length of the mixing path [13] from

$$\eta_T = \rho l^2 |du/dr|,\ \lambda_T = C_p l,\ l_T |du/dr|, \tag{6}$$

where ρ is density, C_p is the specific heat of the plasma, and l and l_T are the mixing path lengths for the transfer of momentum and energy. Here we assume that $l = l_T$. Out of the available semiempirical formulas for the mixing length, we selected three which differ substantially in value:

$$l_1 = 0.4(R - r); \tag{7}$$

$$l_2 = R[0.14 - 0.08(r/R)^2 - 0.06(r/R)^4]; \tag{8}$$

$$l_3 = \begin{cases} 0.4(R-r), & R \geqslant r \geqslant 0.8125R, \\ 0.075R, & 0 \leqslant r \leqslant 0.8125R, \end{cases} \tag{9}$$

where l_1 and l_2 are from [13] and l_3 is from [14].

Integration of (3) and (6) gives the following formulas for η_T and λ_T:

$$\eta_T = \frac{\eta}{2}\left(\sqrt{1 + \frac{2\rho l^2 r}{\eta^2}\left|\frac{dp}{dz}\right|} - 1\right),\quad \lambda_T = C_p \eta_T.$$

System (1)-(3) with the boundary conditions of (4) and (5) is solved numerically. As l is independent of the plasma speed, (1) and (2) were solved without reference to the equation of motion. The electric field strength and the static-pressure gradient were taken as parameters, while the dynamic viscosity, C_p, and W_r were given by tables from the data of [3, 7, 15]. A finite-difference method was used with iteration. At each step the linearized system of algebraic equations was solved by the pivot method. The iteration ended when the following condition was obeyed:

$$\left|(T_0^{k+1} - T_0^k)/T_0^k\right| \leqslant \varepsilon = 0.001,$$

where k is the number of the iteration and T_0 is the axial temperature. When the temperatures had been found, the equation of motion was solved by the pivot method and then the integral characteristics were calculated: the arc current $I = 2\pi E \int_0^R \sigma r dr$ and the mass flow rate $G = 2\pi \int_0^R \rho u r dr$. The calculations were checked from the obedience to the integral energy balance condition for the entire channel. Another algorithm was used to estimate the re-

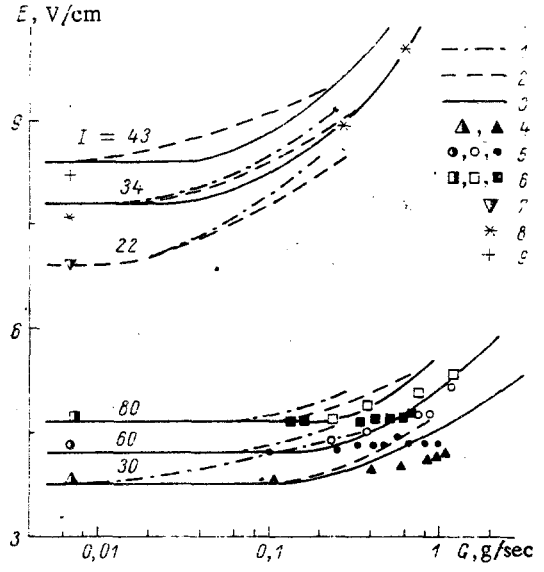

Fig. 1

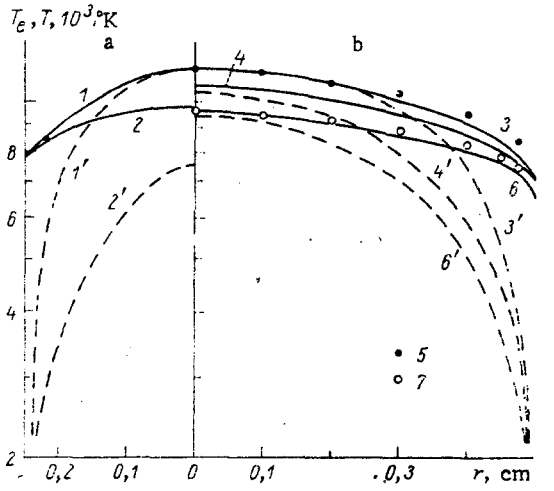

Fig. 2

liability of the data: the finite-element method [16]. The two methods gave essentially coincident results, which shows that the arc characteristics are calculated reliably.

The electrical and thermal characteristics of the arc most fully reflect the state of the plasma flow. As basic characteristics we took the electric field strength, the temperatures of the electron and atom-ion gases, and the heat-flux densities.

Figure 1 shows the effect of gas flow rate on the field strength for two channel radii: R = 0.25 cm for arc currents I = 22, 34, and 43 A and R = 0.5 cm with arc currents I of 30, 60, and 80 A. We calculated the field strengths with the three formulas of the mixing length (curves 1 from (7), 2 from (8), and 3 from (9)), and these were compared with experiment for the corresponding arc currents: *4* — $I = 30$ A, *5* — $I = 60$ A, *6* — $I = 80$ A, *7* — $I = 22$ A, *8* — $I = 34$ A, *9* — $I = 43$ A , where the half-filled points are the data from [17], the open points are from [19], and the filled points are from [18], while the points in the form of crosses and stars are our experimental data obtained on a plasmotron with inserts between the electrodes. At gas flow rates less than a certain value G*, the electric field strength calculated from any of the formulas (7)-(9) was constant, which corresponds to laminar flow. In this region of gas flow rates, the calculations agreed well with experiment. The value of G* increases with the radius of the discharge channel; for example, $G^* \approx 0.04$ g/sec for R = 0.25 cm and $G^* \approx 0.3$—0.4 g/sec for R = 0.5 cm. The electric field strength increases if the flow rate exceeds G*. The best agreement with experiment is given by (9), when a comparison is made with (7) and (8).

Change in the mixing length affects factors other than the electric field. Table 1 gives some arc characteristics calculated for R = 0.5 cm from (7)-(9), which shows that (9) gives the highest values for the electron temperature T_{e0}, the electron temperature averaged over the cross section $\langle T_e \rangle$, and the temperature $\langle T \rangle$ of the atom-ion gas, and also of the current when a comparison is made with (7) and (8), Also, the turbulent flow has marked effects on the magnitude and distribution of the plasma temperature but little effect on the speed. On this basis, the subsequent calculations were based on (9) for the mixing length as giving the best agreement with experiment.

The characteristic radial temperature distributions for the electrons (solid lines) and the atom-ion gas (broken lines) are shown in Fig. 2 for two channel radii (a — R = 0.25 cm, b — R = 0.5 cm); curves 1, 1' (G = 0.05 g/sec, I = 40 A), 3, 3' (G = 0.26 g/sec, I = 100 A) and 6, 6' (G = 0.05 g/sec, I = 41 A) correspond to laminar flow, while curves 2, 2' (G = 1.63 g/sec, I = 40 A) and 4, 4' (G = 2.3 g/sec, I = 100 A) correspond to turbulent. The calculated electron-temperature profiles (curves 3 and 6) agree well with experimental data obtained by others: 5 — G = 0.23 g/sec, I = 100 A [2] and 7 — G = 0, I = 35 A [15]. As the current increases (curves 6-6' and 3-3'), or as the radius decreases (curves 1-1' and 3-3'), the temperature gradients increase. No matter what the channel size, the atom-ion gas is cooled more extensively than the electron one as the gas flow rate increases. On transition

TABLE 1

dp/dz, Pa/cm	E, V/cm	l	T_{e0}, °K	$\langle T_e \rangle$, °K	$\langle T \rangle$, °K	I, A	G, g/sec	u_0, m/sec
5	4,2	l_1	10 080	8580	6700	56	0,05	14
		l_2	10 330	8640	6900	60	0,04	14
		l_3	10 400	8780	6980	61	0,04	14
	4,8	l_1	10 060	9310	7910	89	0,04	13
		l_2	11 110	9220	7730	86	0,03	13
		l_3	11 190	9390	7960	91	0,04	14
100	5,4	l_1	10 320	9000	7360	88	0,43	129
		l_2	10 790	9140	7520	93	0,47	159
		l_3	11 200	9400	7920	102	0,44	172

to turbulent flow, the temperature profiles become flatter and the region of thermal disequilibrium extends to the entire discharge channel.

The radial position of the boundary for substantial thermal disequilibrium $(r/R)_n$ is characterized by a difference between T_e and T nominally taken as 300°K [20], and this is shown in Fig. 3 as a function of channel radius, where 1, 2, 5, and 6 are for I = 100 A and 3, 4, and 7 are for I = 60 A, with 1 and 3 for G = 0 and the other calculated curves (2 and 4) and the experimental ones (5 and 7 from [6, 20] and 6 from [20]) are for G = 0.1 g/sec. It is clear that an arc in a channel of larger radius is thermally closer to equilibrium (Fig. 2). The disequilibrium is increased by raising the gas flow rate and reducing the current. The calculated position of the boundary for substantial thermal disequilibrium for G = 0.1 g/sec agrees well with estimates [20] for I = 60 and 100 A, namely correspondingly points 7 and 5, 6 in Fig. 3. The slopes of the curves 1-4 indicate the rate of increase in the thermal disequilibrium as the radius varies. Figure 3 shows that this rate is the larger the lower the arc current.

Figure 4 also shows the thermal disequilibrium, where we have calculated the electron temperature $\langle T_e \rangle$ averaged over the cross section (solid lines) and the same for the atom-ion gas $\langle T \rangle$ (broken lines) for the following conditions: 1 — 1' — R = 0.5 cm, dp/dz = 50 Pa/cm, G = 0.24—0.3 g/sec; 2 — 2' — R = 0.5 cm, dp/dz = 1000 Pa/cm, G = 1.7—3.5 g/sec; 3 — 3' — R = 0.25 cm, dp/dz = 1000 Pa/cm, G = 0.22—0.53 g/sec; 4 — 4' — R = 0.25 cm, dp/dz = 10,000 Pa/cm, G = 1.3—1.9 g/sec. The average electron temperatures are in good agreement with experiment (points 7-9) from [21-23] correspondingly, particularly for R = 0.5 cm. On the other hand, the average temperatures of the atom-ion gas as indicated by the calculations (curves 1'-2' and 3'-4') differ somewhat from the experimental values 5-5' and 6-6' obtained in [24] for channels of radius 0.3 and 0.5 cm correspondingly, with 5 and 6 for G = 0.25 g/sec and 5' and 6' for G = 1.2 g/sec. Also, the calculated range in the atomic-ionic gas temperature in relation to flow rate is somewhat smaller than that indicated by experiment, which is evidently due to inadequacy in the semiempricial formula (9), which does not incorporate features of the arc burning, namely pulsations, oscillations, and various instabilities in the conducting part. If we use (7) or (8) to calculate the mixing length, the discrepancies from experiment become larger (Table 1). However, the error in measuring the electron temperatures is ±500°K, while that for the atom-ion one is ±1000°K, so one can say that there is satisfactory agreement between the calculated and experimental data.

Figure 5 compares the effects of various factors on the arc characteristics over a wide range in gas flow rate, which shows the densities of the heat fluxes due to atom-ion thermal conduction $(1—1' — q_a = \lambda dT/dr)$, turbulent thermal conduction $(2—2' — q_T = \lambda_T dT/dr)$, electron thermal conduction $(3—3' — q_e = \lambda_e dT_e/dr)$ ionization-energy transport by ambipolar diffusion $\left(4 — 4' — q_d = \left(\frac{3}{2} kT_e + E_i\right) D_a \frac{dn_e}{dr}\right)$, and energy transfer by radiation $\left(5 — 5' — q_\Pi = \frac{1}{r}\int_0^r W_r r dr\right)$ as calculated for r = 0.5 R for two channel radii: $R = 0.25$ cm, $\langle j \rangle = 250$ A/cm^2, broken lines and $R = 0.5$ cm, $\langle j \rangle = 115$ A/cm^2, solid lines. At gas flow rates less than 0.1 g/sec, the tur-

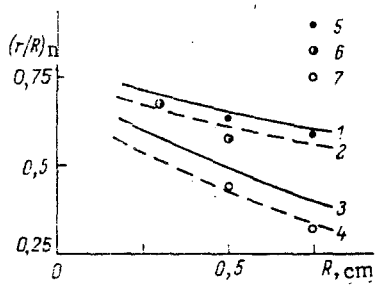

Fig. 3

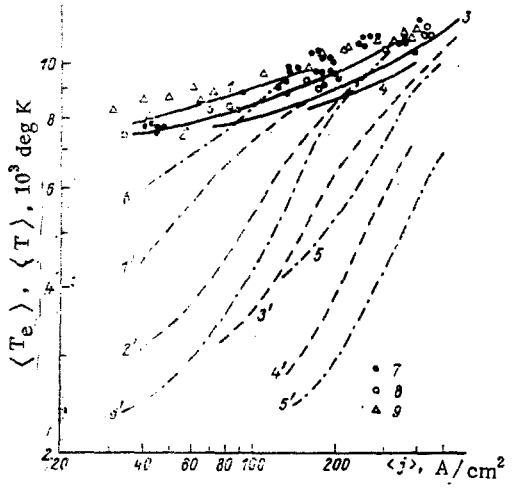

Fig. 4

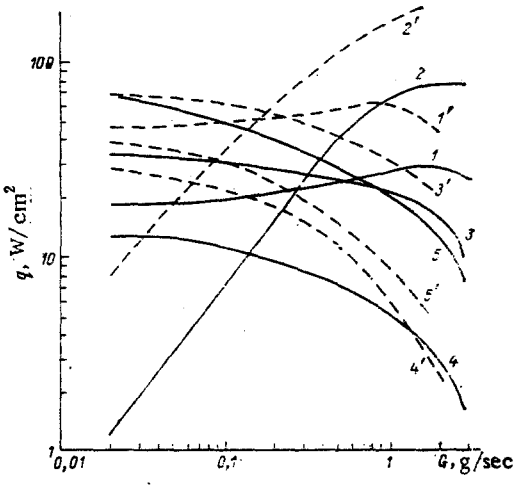

Fig. 5

turbulent heat transport is much less than that due to other mechanisms responsible for transferring energy to the channel wall, and it does not have an appreciable effect on the plasma characteristics. In fact, the electric field strength is independent of the gas flow rate in this range (Fig. 1). The nonzero turbulent heat transport with laminar gas flow has no effect on the radial electron-temperature distribution (Fig. 2) calculated for G = 0.05 g/sec and I = 41 A (curve 6), which agrees well with experiment. The energy transfer due to turbulent thermal conduction becomes important for $G \leqslant 0.2$ g/sec for R = 0.25 cm and for $G \geqslant 0.5$ g/sec for R = 0.5 cm, which corresponds to values of the Reynolds number $Re = 2G/\mu\pi R$ calculated from the viscosity of the cold gas at the wall of 2320 and 2900, which agrees well with the range of Reynolds numbers characterizing the transition from laminar to turbulent flow.

The effects of turbulent heat transfer increase with the gas flow rate and are most pronounced for the temperature of the atom-ion gas, as is clear from Fig. 4, where curves 2-2' and 4-4' characterize T_e and T in turbulent flow, while curves 1-1' and 3-3' characterize these in the flow transitional from laminar to turbulent. Here we should note that the reductions in electron and atom-ion temperatures due to increase in the turbulent transport reduce the heat fluxes due to electron thermal conduction and energy transport by ionization and radiation. The slight rise in q_a with G occurs because the increase in the gradient of the atom-ion gas temperature is larger than the reduction in the atom-ion thermal conductivity.

This study has provided good agreement between the calculated and experimental data on laminar and turbulent flow in an arc channel. Turbulence in the flow has its most marked effect on the electric field strength and on the temperature of the atom-ion gas, with a smaller effect on the electron temperature. Turbulent heat transport becomes important relative to the molecular mechanism at Reynolds numbers of 2300-2900 as calculated for the cold gas. This agrees well with the data for slightly heated flows in tubes. In accordance with the above, this model for an arc in a turbulent gas flow can be used to calculate the characteristics of the steady-state flow for a two-temperature argon-arc plasma in a channel.

LITERATURE CITED

1. A. D. Lebedev, "Electron-temperature deviation in a dense argon plasma," Izv. Sib. Otd. Akad. Nauk SSSR, No. 10, Ser. Tekhn. Nauk. Issue 3 (1966).
2. K. J. Clark and F. P. Incropera, Thermochemical Nonequilibrium in an Argon Constructed Arc, AIAA Paper No. 71-593 (1971).
3. S. V. Dresvin, A. V. Donskoi, V. M. Gol'dfarb, and V. S. Klubnikin, Physics and Engineering of Low-Temperature Plasma [in Russian], Atomizdat, Moscow (1972).
4. S. V. Dresvin, "A two-temperature plasma model under conditions of steady-state gas flow through a plasmotron," Zh. Prikl. Mekh. Tekh. Fiz., No. 4 (1973).
5. I. P. Nazarenko and I. G. Panevin, "Calculating the characteristics of a weakly ionized arc with allowance for radiation transport and temperature differences," in: Simulation and Calculation Methods for Physicochemical Processes in Low-Temperature Plasma [in Russian], Nauka, Moscow (1974).
6. A. I. Ivlyutin, "Disequilibrium phenomena in stabilized arcs," in: Proceedings of the Seventh All-Union Conference on Low-Temperature Plasma Generators [in Russian], Vol. 2, Alma Ata (1977).
7. R. S. Devoto, "Transport coefficients of partially ionized argon," Phys. Fluids, 10, 354 (1967).
8. V. N. Kolesnikov, "An arc discharge in an inert gas," Trudy FIAN, Fiz. Opt., 30, 66 (1964).
9. T. K. Bose, "Anode heat transfer for a flowing argon plasma at elevated electron temperature," Int. J. Heat Mass Transfer, 15, No. 10 (1972).
10. L. Spitzer, Physics of Completely Ionized Gases [Russian translation], Mir, Moscow (1965).
11. W. Finkelnburg and H. Mecker, Electric Arcs in Thermal Plasma [Russian translation], Inostr. Lit., Moscow (1961).
12. V. L. Granovskii, Electric Current in Gases [in Russian], Nauka, Moscow (1971).
13. K. K. Fedyaevskii, A. S. Ginevskii, and A. V. Kolesnikov, Calculating the Turbulent Boundary Layer in an Incompressible Fluid [in Russian], Sudostroenie, Leningrad (1973).
14. M. P. Escudier and D. B. Spalding, A Note on the Turbulent Uniform-Property Boundary Layer on a Smooth Impermeable Wall, ARCC Paper No. 875 (1965).
15. J. F. Bott, "Spectroscopic measurement of temperature in an argon plasma arc," Phys. Fluids, 9, No. 8 (1966).
16. L. J. Segerlind, Applications of the Finite-Element Method [Russian translation], Mir, Moscow (1979).
17. H. W. Emmons, "Arc measurement of high-temperature gas transport," Phys. Fluids, 10, No. 6 (1967).
18. P. W. Runstadler Jr., The Laminar and Turbulent Flow of an Argon Arc Plasma, AIAA Paper, No. 66-189 (1966).
19. A. V. Donskoi, V. S. Klubnikin, and A. S. Parkhomenko, "An experimental study of the electrical and thermal characteristics of stabilized arcs," Inzh.-Fiz. Zh., 22, No. 6 (1972).
20. É. I. Asinovskii, E. P. Pakhomov, and I. M. Yartsev, "A study of the characteristics of the laminar flow of an argon plasma in an electric arc," in: Chemical Reactions in Low-Temperature Plasma [in Russian], INKhS im. A. V. Topcheva, Moscow (1977).
21. V. S. Klubnikin and A. S. Parkhomenko, "Results on the energy characteristics of an argon arc in a sectional plasmotron," in: Abstracts for the Fifth All-Union Conference on Low-Temperature Plasma Generators [in Russian], Vol. 1, ITF Sib. Otd. Akad. Nauk SSSR, Novosibirsk (1972).
22. V. A. Baturin, "Experimental determination of the electrical conductivity of an argon plasma in a stabilized arc," Zh. Prikl. Mekh. Tekh. Fiz., No. 2 (1970).
23. H. W. Emmons, "A study of heat transfer in a plasma," in: Current Problems in Heat Transfer [in Russian], Energiya, Moscow–Leningrad (1966).
24. A. V. Donskoi and V. S. Klubnikin, Electrical Plasma Processes and Apparatus in Engineering [in Russian], Mashinostroenie, Leningrad (1979).